RESEARCH FRONT

CSIRO PUBLISHING

Aust. J. Chem. **2016**, *69*, 573–582
http://dx.doi.org/10.1071/CH15779

Full Paper

Experimental and Computational Studies of the Mechanisms of Hydroamination/Cyclisation of Unactivated α,ω-Amino-alkenes with CCC-NHC Pincer Zr Complexes*

Wesley D. Clark,[A,B] *Katherine N. Leigh,*[C] *Charles Edwin Webster,*[A,C,D] *and T. Keith Hollis*[A,B,D]

[A]Department of Chemistry, Mississippi State University, Mississippi State, MS 39762, USA.
[B]Department of Chemistry and Biochemistry, The University of Mississippi, Oxford, MS 38655, USA.
[C]Department of Chemistry, The University of Memphis, Memphis, TN 38152, USA.
[D]Corresponding authors. Email: ewebster@chemistry.msstate.edu; khollis@chemistry.msstate.edu

Four new CCC-NHC pincer Zr complexes have been synthesised, characterised, and used in mechanistic studies in the hydroamination/cyclisation of unactivated amino-alkenes. These Zr pre-catalysts will cyclise a primary amino-alkene, but no reaction was observed for a secondary amino-alkene even in the presence of a primary amine. The empirical rate law, experimentally determined activation parameters, and kinetic isotope effects (KIEs) are reported. Several possible mechanisms, including amido- versus imido-insertion and concerted-insertion versus [2 + 2] cycloaddition mechanisms, were modelled computationally at the PBEPBE level of theory with double-zeta quality basis sets. The formation of a catalytically relevant imido complex via the monoamido complexes was accompanied by in situ formation of ammonium salts of the substrates. The experimental and computational data are consistent with an imido-[2 + 2] cycloaddition mechanism for the CCC-NHC pincer diamido Zr complexes that follow saturation kinetics under catalytically relevant concentrations.

Manuscript received: 12 December 2015.
Manuscript accepted: 7 March 2016.
Published online: 11 April 2016.

Introduction

Pyrrolidines and piperidines are important classes of *N*-heterocycles present in many biologically active molecules and pharmaceuticals.[1] Hydroamination/cyclisation of unactivated amino-alkenes is an atom economical pathway to these molecules.[2] However a high activation barrier (~42 kcal mol^{-1}) from electrostatic repulsion due to the amine lone pair and the alkene π-bond prevents the direct reaction from occurring without a catalyst.[3] A wide variety of hydroamination/cyclisation catalysts have been reported incorporating chiral or achiral ligands, and transition or rare earth metals.[4] Accordingly, several mechanistic pathways have been proposed.[4b,4f,5] The amido insertion mechanism (Scheme 1a) has been reported for organoactanides which catalyse hydroamination/cyclisation of primary and secondary amino-alkenes.[5a] Two concerted proton transfer mechanisms have been reported. Scheme 1b, the amine-enhanced amido insertion mechanism, and Scheme 1c, the amido-enhanced amido insertion mechanism, illustrate simplified versions of the mechanisms reported by Schafer et al. and Sadow et al. respectively.[4b,5d] An imido-[2 + 2] cycloaddition mechanism has also been reported (Scheme 1d) for group 4 complexes, which have not been reported to catalyse hydroamination/cyclisation of secondary amino-alkenes.[4c,4f] Computational only studies have also been reported.[6] Some of us recently reported CCC-NHC pincer Zr complexes and their hydroamination/cyclisation activity, particularly that the diamido complexes (see preceding paper[7]) are faster than the monoamido complexes in contrast to reports by others.[5a] A synergistic rate enhancement with the addition of a CCC-NHC pincer triiodo Zr complex was recently reported.[8] Herein, we report mechanistic studies on the hydroamination/cyclisation of unactivated amino-alkenes with CCC-NHC pincer Zr complexes employing experimental and computational techniques.

*Dedicated to the memory of Professor B. Bosnich and the clarity of thought he brought to the most significant problems.

Results and Discussion

Synthesis and Characterisation of CCC-NHC Pincer Zr Complexes

Initial attempts to perform kinetic runs with the previously reported butyl derivatives at the lower temperatures needed for NMR observations led to the observation of heterogeneous mixtures (see below). Therefore, derivatives with longer alkyl chains were prepared (Scheme 2), which provided improved solubility. The imidazolium salts **1b** (*n*-hexyl) and **1c** (undecyl) were synthesised in a manner similar to the previously reported synthesis of imidazolium salt **1a**. Imidazolium salts **1b** and **1c** were reacted with 1.1 equiv. of $Zr(NMe_2)_4$ yielding diiodo complexes **2b** and **2c**. Imidazolium salt **1a** was reacted with 2.5 equiv. of $Zr(NMe_2)_4$ yielding diamido complex **4a** as a crystalline solid (Scheme 2). Furthermore, triiodo complex **3c** was synthesised by reacting undecyl imidazolium salt **1c** with 1.1 equiv. of $Zr(NMe_2)_4$ and then excess MeI. The characteristic imidazolium peak (10–12 ppm) was not observed in the ^1H NMR spectrum for each of the complexes. The ^{13}C NMR spectra of the complexes contain a $^{13}C_{NHC}$ resonance near 190 ppm. These data are consistent with the formation of CCC-NHC pincer Zr complexes. Complexes **2b**, **2c**, **3c**, and **4a** were isolated as analytically pure solids despite their sensitivity to moisture.

Preliminary Evaluation of a New CCC-NHC Zr Complex for Activity in Hydroamination/Cyclisation

Initial kinetic trials using the previously reported butyl-CCC-NHC pincer Zr complexes (**2a** or **3a**) in C_6D_6 or toluene-d_8 resulted in heterogeneous mixtures with solids present at temperatures where a lock signal was obtainable. Homogeneous solutions were observed at higher temperatures near the previously reported catalytic temperature of 160°C, but the solutions were refluxing in the NMR tube and a lock signal was not obtainable. However, homogenous systems were obtained for the diiodo complexes **2b**, **2c**, and diamido complex **4a** when 1,2-dichlorobenzene was used as the solvent. Despite the incorporation of undecyl substituents into complex **3c**, catalytic trials remained heterogeneous. Complexes **2b**, **2c**, **3c**, and **4a** were evaluated for their activity in the hydroamination/cyclisation of standard, unactivated α,ω-amino-alkenes (Table 1). Results from these catalytic trials are summarised in Table 1. All four complexes efficiently converted primary amino-alkene substrate **5** into a cyclised product (entry 1).

A trace quantity of the oxidative amination product **8**[9] was observed when amido complexes **2b**, **2c**, and **4a** were employed. Curiously, the amount of oxidative amination product observed was near the catalyst loading levels, which is consistent with its formation being part of a catalyst decomposition pathway. However, oxidative amination product **8** was not observed when using triiodo complex **3c**. Such an observation is consistent with the dimethyl amido ligand contributing to the decomposition. When secondary amine substrate **6** was evaluated with each pre-catalyst, no reaction was observed (Table 1, entry 2). The addition of an exogenous, un-cyclisable primary amine while attempting to cyclise secondary amino-alkene **6**, did not provide any conversion (Table 1, entry 2, footnote B). Thorough evaluation of other CCC-NHC pincer Zr complexes as pre-catalysts for the hydroamination/cyclisation of primary amino-alkenes has already been reported.[8a,8c] The results in Table 1 are consistent with CCC-NHC pincer Zr complexes **2b**, **2c**, **3c**, and **4a** as active pre-catalysts for the hydroamination/cyclisation of primary amino-alkenes in line with prior reports.

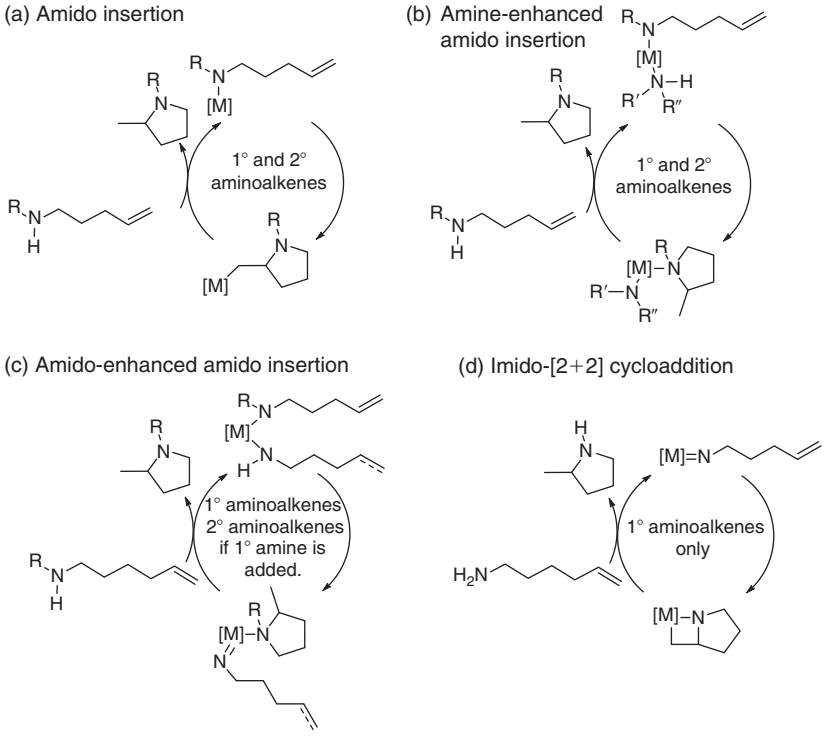

Scheme 1. Key transition state elements for reported hydroamination/cyclisation mechanisms: (a) Amido insertion.[5a] (b) Amine-enhanced amido insertion.[4b] (c) Amido-enhanced amido insertion with imido formation.[5d] (d) Imido-[2 + 2] cycloaddition.[4c]

Computational Modelling of Potential Mechanisms with CCC-NHC Pincer Zr Complexes

While experimental and computational studies were occurring simultaneously, the results of the computational studies are presented first to establish the scope of potential mechanisms.

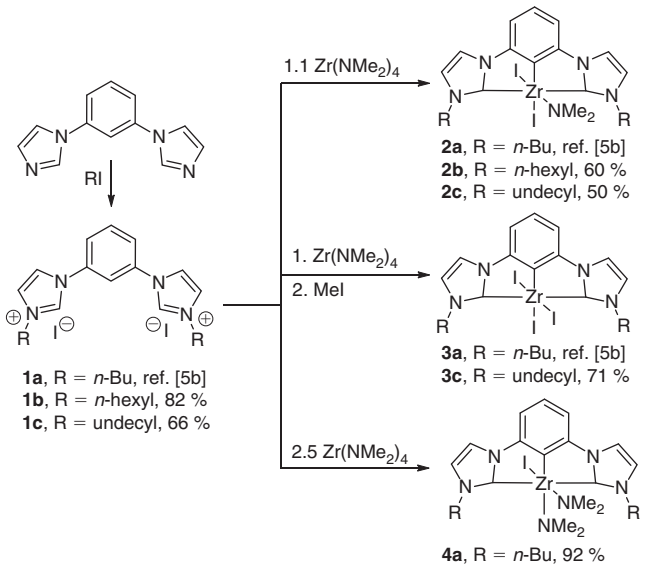

Scheme 2. Synthesis of imidazolium salts (**1a**–**c**) and CCC-NHC pincer Zr complexes used in these studies.

Table 1. Evaluation of complexes 2b, 2c, 3c, and 4a as pre-catalysts for hydroamination/cyclisation

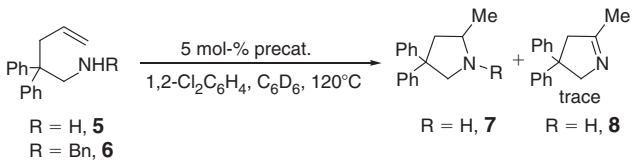

Entry	R	Conv. [%], time [h], **7**:**8**[A]			
		2b	**2c**	**3c**	**4a**
1	H	>98, 3, 35:1	>98, 3, 33:1	>98, 2[C,D], –	>98, 2, 16:1
2	Bn	0, 12[B]	0, 12[B]	0, 12[B]	0, 12[B]

[A]Conversion and **7**:**8** ratio determined by ^{1}H NMR spectroscopy.
[B]Adding 20 mol-% *n*-hexylamine and heating for 24 h at 120°C resulted in 0 % conversion (no reaction).
[C]Heterogenous (solid present).
[D]Formation of **7a** was not observed.

Multiple reaction pathways were considered, and each was modelled computationally at the PBEPBE level of theory with the LANL2DZ basis set. The alkyl groups on the imidazolyl ring and the phenyl groups on the substrate were truncated to methyl groups. Not all potential mechanisms as outlined in Scheme 1 were investigated or reported due to simple scope and limitations of the catalysis eliminating these possibilities.

CCC-NHC Pincer Zr Complex Disproportionation/ Conproportionation – Experiment and Computation

The working hypothesis (as described in the preceding paper) based on no reaction with secondary amines and the qualitative catalyst concentration experiments was that the monoamido complex **2a** effectively disproportionated to give a bis-amido complex **4a** as illustrated in Scheme 3, which was necessary for catalysis (imido formation), with concomitant formation of a triiodo complex **3a**. Consistent with this hypothesis was the observation of complete loss of catalytic activity below a threshold concentration. The computed free energies of the species involved in the proposed disproportionation are also included in Scheme 3, and predict a ΔG°_{rxn} of + 4.6 kcal mol^{-1}, which is consistent with the experimental observation of no observable disproportionation of the mono-amido complex **2a** in solution. For computational simplicity the butyl group was replaced with a methyl group, as this change was expected to have little to no impact on the computed results. In addition, when diamido complex **4a** was mixed with triodide complex **3a** (Scheme 3, reverse reaction) at room temperature immediate conproportionation was observed to produce the monoamido complex **2a** (see Figs S24 and S25 in the Supplementary Material). Although little diamido **4a** would be expected to be generated in solution starting from mono-amido **2a**, the diamido complex **4a** was stable when prepared independently.

Amido Insertion Mechanism

This well known mechanism was examined for CCC-NHC pincer Zr complexes and is illustrated in Scheme 4, since it would require only one amido ligand as found in catalytically active **2a**.[8b,8c] Simple ligand exchange from pre-catalyst **4** yields intermediate **9**, which may be described as the 'catalytically active species' in this cycle. There are two key high energy transition states in the proposed pathway – the insertion and protonation steps. The insertion of the alkene into the Zr–N bond of intermediate **9** through **TS-9**–**10** with $\Delta G^\ddagger$ = 22.3 kcal mol^{-1} yields intermediate **10**. Throughout the discussion **TS-9**–**10** (or, generally, **TS-X-Y**) is used to indicate the highest transition state from intermediate **9** to intermediate **10**. But, to be clear, it may not represent a single step on the potential energy surface (PES). Intramolecular proton transfer (**TS-10**–**11**, Scheme 4)

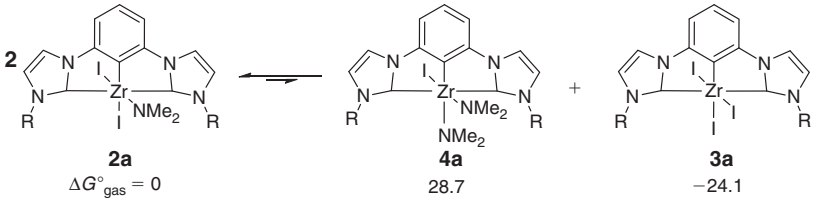

Scheme 3. Computed free energies for the disproportionation of mono-amido CCC-NHC pincer Zr complex in the gas phase. Computations were performed with R = Me. Experimental results were obtained with R = Bu. The relative free energies presented in this scheme are for an internally consistent comparison only and do not correlate with the values below.

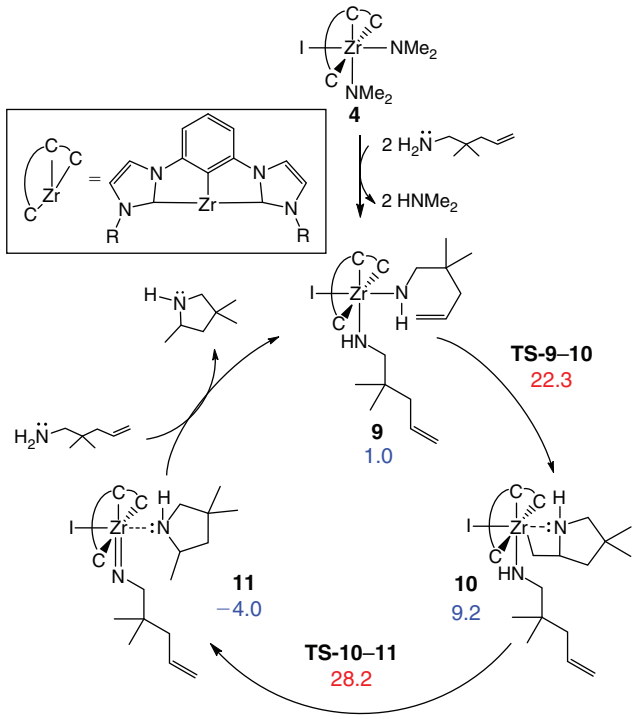

Scheme 4. Computationally modelled amido insertion mechanism for CCC-NHC pincer Zr complexes. Relative energies (ΔG°) of intermediates **9**, **10**, and **11** are given and the free energy of activation of the key transition states are also included.

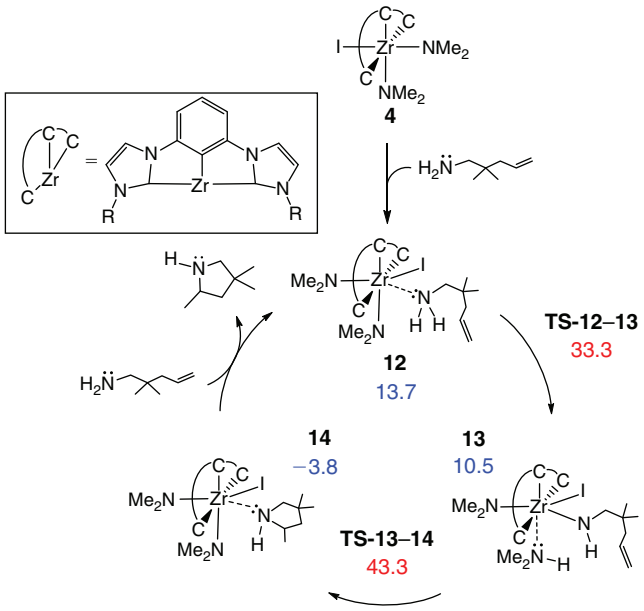

Scheme 5. Computationally modelled amine-enhanced concerted amido mechanism with expanded coordination number. Relative energies (ΔG°) of intermediates **12**, **13**, and **14** are given, and the energies of the transition states are also included.

has a higher free energy of activation ($\Delta G^{\ddagger} = 28.2$ kcal mol^{-1}) leading to imido intermediate **11**, which regenerates catalytically active **9** upon product dissociation and substrate addition with concomitant proton transfer.

If this mechanism were operative, secondary amino-alkenes would be expected to cyclise in the presence of a primary amine, in a manner similar to that reported by the Sadow group.[5d] An un-cyclisable primary amine is required as a proton shuttle for secondary amine substrates in this mechanism. The density functional theory (DFT) studies are clearly consistent with a large free energy of activation for this pathway in the current catalyst system. No reaction was observed with secondary amines as was previously reported,[8c] not even in the presence of a primary amine as documented in Table 1, entry 2, footnote B (see above). Therefore, it seems unlikely that the amido insertion mechanism is operative in CCC-NHC pincer Zr complex catalysed reactions.

Amine-Enhanced Concerted-Proton Transfer Amido Mechanism with Expanded Coordination Sphere

Zr is well known to expand its coordination sphere. For example, Cp_4Zr is considered 10-coordinate as it has three η^5-Cp (Cp = cyclopentadiene) rings, each occupying three coordination sites, and one η^1-Cp.[10] No evidence for higher-coordination numbers have been observed in the CCC-NHC pincer complexes. However, because many reports of the early transition metal catalysed hydroamination involve Cp ligands and higher coordinate Zr (typically seven-coordinate) in the catalytic cycle, expansion to a seven-coordinate species was examined computationally. The results are illustrated in Scheme 5. Intermediate **12** was formed by coordination of a substrate molecule with subsequent proton transfer producing seven-coordinate intermediate **13**, which has a Zr–I distance of 3.27 Å. The free energy of the transition state for this 1,3 proton transfer between nitrogen atoms was computed to be +33.3 kcal mol^{-1}, a prohibitively high value. And yet, the next step with concurrent C–N and C–H bond formation has an even higher free energy of activation of +43.3 kcal mol^{-1} on the path to **14**. If the CCC-NHC pincer Zr complexes employed this type of mechanism, secondary amino-alkenes should be cyclised. The lack of cyclisation observed for secondary amino-alkenes[8a,8c] and the high free energies of activation that were computed suggest that this mechanism is not involved for the CCC-NHC pincer Zr catalysed reactions.

Concerted Imido-[2 + 2] Cycloaddition

This mechanism was also computationally modelled as illustrated briefly in Scheme 6 (see the Supplementary Material for a detailed principle of the microscopic reversibility model of this mechanism). The lack of cyclisation for a secondary amino-alkene, even in the presence of a primary amine (Table 1, see above) was consistent with the formation of a catalytically relevant imido intermediate **15**. The concentration corrected energy for **15** is 3.4 kcal mol^{-1} lower than the diamido pre-catalyst **4**. The imido intermediate **16** is predicted to undergo cyclisation through a low energy transition state (**TS-16–17**, $\Delta G^{\ddagger}_{comp} = +14.0$ kcal mol^{-1}) producing azazirconacyclobutane **17** in a reaction step that is initially exergonic by 6.4 kcal mol^{-1} (see Fig. S48, Supplementary Material). When the substrate is included the energy rises to 12.9 kcal mol^{-1} as indicated for **17** in Scheme 6. Coordination of the substrate is exergonic by 6.8 kcal mol^{-1} (**17** versus **18**). The proton transfer from N to C producing intermediate **19** is predicted to be the turnover limiting step with a transition state (**TS-18–19**) free energy of activation of +18.1 kcal mol^{-1}, which is the highest computed transition state value in a highly exergonic process that is attributable to the seven-coordinate intermediate going to six coordinate plus the C–H bond formation.

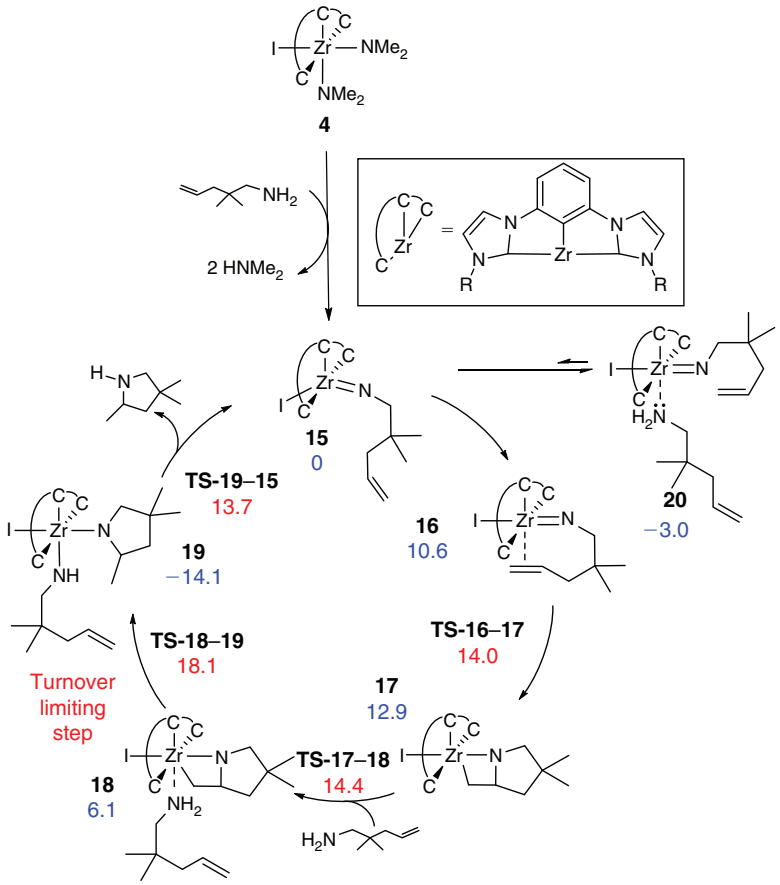

Scheme 6. Computationally modelled [2 + 2] cycloaddition mechanism. Relative energies (ΔG°) of intermediates **15**–**20** are given, and the energies of the transition states are also included.

Intermediate **19** is predicted to undergo proton transfer and loss of product in an overall endergonic step to yield five-coordinate intermediate **15**. Furthermore, it was predicted that coordination of the alkene to regenerate the 'catalytically active species' **15**, is endergonic by +14.1 kcal mol^{-1}. This prediction, that the five-coordinate intermediate **15**, which is a 16-electron complex with π-donation from the iodo ligand, is more stable than the six-coordinate intermediate **16**, which is a 16-electron complex (four electrons from iodo, six from CCC-NHC, two from alkene, and four from the 'bent' imido), is consistent with the requirement of the gem-dialkyl effect for efficient cyclisation, and the lack of reactivity towards intermolecular hydroamination of alkenes. The origin of the preference 'not to coordinate the alkene' may be found in the requirement of the imido to bend for alkene coordination, and that the trigonal bipyramidal configuration avoids two disfavoured trans-influence interactions, namely, the *trans*-I–imido and the *trans*-C^{Ar}–alkene. If the primary cause of the preference was the imido bending then there would be little impact expected on the intermolecular reaction, therefore the inference is that the octahedral geometry at Zr required to assemble all of the 'substrates' is disfavoured in the ligand set and coordination environment. It was also found computationally that the substrate should strongly inhibit the reaction by coordinating to the catalytically active species **15** to generate **20**. The equilibrium is predicted to strongly favour the bound substrate complex, which impacts the reaction rates and order in the substrate. If this mechanism was operative, the following predictions should hold: 1) A primary kinetic isotope effect should be measureable. 2) Considering the highly ordered state (catalyst, bicyclic intermediate, and an additional molecule of substrate for protonation) for the conversion of **18** into **19** a large negative $\Delta S^{\ddagger}$ value would be anticipated. 3) Only primary amines will cyclise. 4) Intermediate **18** would be the potential resting state of the catalyst. The experimental data presented below are most consistent with the imido-[2 + 2] cycloaddition mechanism being operative for CCC-NHC pincer Zr catalysed hydroamination cyclisation.

Pre-Catalyst Stability: ^{1}H NMR Investigations

*Mono-Amido **2b***

The possibility of pre-catalyst decomposition was investigated for diiodo complex **2b**. When diiodo complex **2b**, primary substrate **5**, and toluene-d_8 were combined at room temperature a homogenous yellow solution was formed that contained no resonances attributable to an imidazolium salt (no resonances at >8.5 ppm in the ^{1}H NMR spectrum). However, after sitting at room temperature for 30 min or heating at 100°C, a precipitate was observed. Upon dissolving the precipitate with CD_2Cl_2, resonances were observed in the ^{1}H NMR spectrum that were consistent with imidazolium salt formation. However, when the reaction was performed in 1,2-dichlorobenzene/C_6D_6 at temperatures >80°C the reaction was homogenous and signals consistent with imidazolium salt formation were not observed. A weak, broad resonance was observed at 11.23 ppm, but resonances at 9.04 and 8.56 ppm, which are indicative of the imidazolium salt, were not observed. These data are consistent

with an intact pre-catalyst complex and are not consistent with imidazolium salt formation during catalytic runs under homogenous conditions (1,2-dichlorobenzene/C_6D_6).

In an effort to identify the source of the peak at 11.23 ppm, the reaction was spiked with imidazolium salt **1b**, **5**·HCl, or Bu_2NH·HCl, all of which resulted in the appearance of strong resonances at 11.40, 9.04, and 8.56 ppm. The peak at 11.23 ppm was assigned to the N–H signals of the ammonium salt. Pre-catalyst **2b** decomposed in non-polar solvents such as C_6D_6 and toluene when combined with a primary amino-alkene. Similar observations were made for complex **2c**. In all cases, however, cyclisation still occurs, suggesting that the Zr complexes that are formed from decomposition are catalytically active, or that the CCC-NHC pincer Zr complex **2b** is regenerated at the temperatures of catalysis.

*Diamido **4a***

No resonances at greater than 8.5 ppm were observed in the ^{1}H NMR spectra of catalytic runs using diamido complex **4a** and primary amino-alkene **5**, which suggests no detectable decomposition of the Zr complex. However, the characteristic triplet for the methylene group α to the imidazolyl *N* (4.03 ppm) decreased late in the reaction progress with the growth of a peak at 4.34 ppm, which was assignable to the oxidative amination product **8** (see Fig. S40, Supplementary Material). No resonances corresponding to the imidazolium salt (11.40, 9.04, and 8.56 ppm, in particular) were observed in catalytic trials using diamido complex **4a**. The data were not consistent with the presence of an imidazolium salt from decomposition being present at detectable levels during homogenous catalysis conditions for monoamido or diamido pre-catalysts.

*Tri-iodide **3c***

Enhanced rates of catalysis were recently reported when triodide complex **3a** was combined with mono-amido complex **2a**, an interesting synergistic effect. Because of the limited solubility of the butyl derivatives, complex **3c** with undecyl alkyl groups was prepared. A homogenous solution was obtained at 110°C when the hydroamination/cyclisation experiment was performed with a very dilute initial triiodo complex **3c** concentration ($[\mathbf{3c}]_0 = 0.0016$ M) and 1,2-dichlorobenzene. The high temperature ^{1}H NMR spectrum contained peaks at 11.55, 9.09, and 8.46 ppm, which was consistent with quantitative formation of imidazolium salt **1c** (Scheme 7). Imidazolium salt **1c** was only sparingly soluble in 1,2-dichlorobenzene and was the cause of the heterogeneous nature of the reaction at higher concentrations. However, the reaction was homogenous when using the secondary amine **6** with triiodo complex **3c**, and signals corresponding to the imidazolium salt were not observed. These results were consistent with triiodo complex **3c** decomposing in the presence of a primary amino-alkene, but not a secondary amino-alkene. The 'synergistic' enhancement of rate for hydroamination/cyclisation undoubtedly arose from the unidentified Zr species (Scheme 7) formed from the decomposition of triiodo complex **3c**.

Empirical Rate Law, Kinetic Isotope Effects, and Activation Parameters

Order of Reaction in Substrate and Catalyst

Kinetic experiments were performed to determine an empirical rate law for catalysis with complexes **2c** and **4a** due to their superior solubility characteristics. The initial rate method was

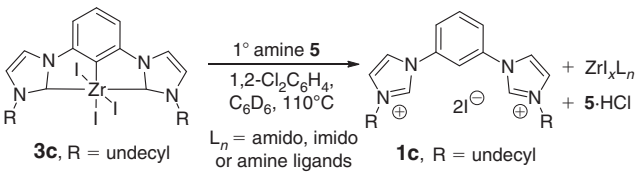

Scheme 7. Reaction observed between triiodo complex **3c** and substrate **5**.

used in an effort to capture the rate of hydroamination/cyclisation before any side reactions occurred. A plot of the natural logarithm of the change in substrate concentration versus time as reflected in the integral with diiodo complex **2c** was found to be linear (see Fig. S44a, Supplementary Material). The linearity of this result is consistent with a first-order dependence upon the amino-alkene **5** (Fig. S44a). When diamido complex **4a** was evaluated with **5** the plot of substrate concentration (as reflected in the integral values) versus time was linear (Fig. S44c, Supplementary Material). Such an observation was consistent with zero-order dependence upon amino-alkene **5** (Figure S44c). This observation is consistent with a reversible coordination of the substrate that is saturated at the relatively high concentrations of the trials before the turnover limiting step (Scheme 6) as has been noted previously for hydroamination.[5d] Each pre-catalyst was independently evaluated over a concentration range. The plot of the k_{obs} values obtained versus the concentration of each is illustrated in Fig. S44b (Supplementary Material) for pre-catalyst **2c**, and in Fig. S44d (Supplementary Material) for pre-catalyst **4a**. The linearity of each plot with an intercept near zero (0) is consistent with a first-order dependence with respect to each pre-catalyst. Therefore the empirical rate laws are:

$$\text{Rate} = k[\mathbf{2c}][\mathbf{5}], \text{ where } k = \text{intrinsic rate constant} \quad (1)$$

$$\text{Rate} = k'[\mathbf{4a}], \text{ where } k' = \text{intrinsic rate constant} \quad (2)$$

Kinetic Isotope Effects (KIEs)

The CCC-NHC pincer Zr catalysts showed normal KIEs when the substrate **5** was prepared with deuterium on nitrogen and cyclised with either **2c** or **4a**. Detailed kinetic plots may be found in the Supplementary Material (Figs S46–S47). When pre-catalyst **2c** was employed a large KIE was found at $k_H/k_D = 4.6 \pm 0.1$ at 110°C. The KIE measured for pre-catalyst **4a** was just over half of that value at $k_H/k_D = 2.4 \pm 0.1$ at 104°C. The slight change in temperature was not expected to have a significant impact. The observation of significant KIEs is indicative of breaking of the N–H bond in the transition state, a common theme in hydroamination/cyclisation.[4b,5a,5d,11]

Activation Parameters

The temperature dependence of the catalysis using complexes **2c** or **4a** was investigated over a range of 20 or 30°C, respectively. The Eyring plot generated from the data is shown in Fig. S45a (Supplementary Material) for complex **2c** and in Fig. S45b (Supplementary Material) for complex **4a**. The $\Delta H^{\ddagger}$ and $\Delta S^{\ddagger}$ values obtained for complex **2c** ($\Delta H^{\ddagger} = 8.7 \pm 0.2$ kcal mol^{-1}, $\Delta S^{\ddagger} = -41 \pm 1$ eu) and **4a** ($\Delta H^{\ddagger} = 8.3 \pm 0.3$ kcal mol^{-1}, $\Delta S^{\ddagger} = -41 \pm 1$ eu) were within experimental error of each other, and were close to the range of values previously reported, but with some differences. The values of $\Delta H^{\ddagger}$ were significantly

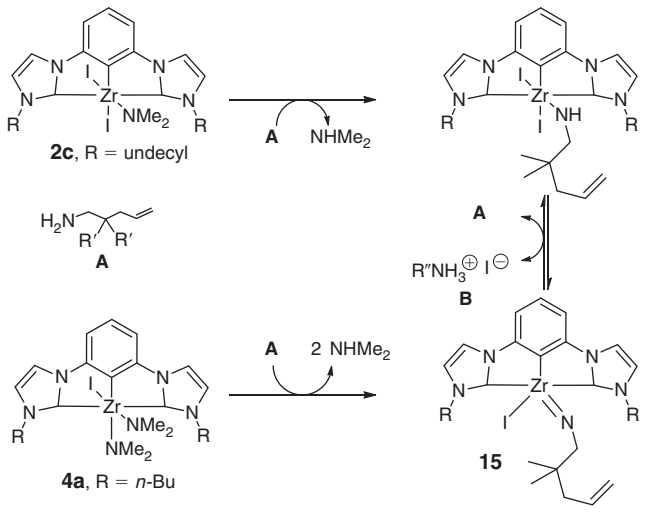

Scheme 8. Generating the catalytically active species from different pre-catalysts.

lower than for $Ti(NMe_2)_4$ ($\Delta H^{\ddagger} = 26.2 \pm 0.7$ kcal mol^{-1}).[11a] They were also lower than values determined for a tetravalent U pre-catalyst ($\Delta H^{\ddagger} = 13.8 \pm 0.3$ kcal mol^{-1}),[11b] and for a Zr salicyloxazoline complex ($\Delta H^{\ddagger} = 17$ to 21 kcal mol^{-1}).[4f] The $\Delta H^{\ddagger}$ values obtained for complexes **2c** and **4a** were similar to values obtained for a Zr cyclopentadienylbis(oxazolinyl)borate complex ($\Delta H^{\ddagger} = 6.7 \pm 2$ eu).[5d] However, the $\Delta S^{\ddagger}$ values obtained for the CCC-NHC Zr complexes **2c** and **4a** were significantly higher than values reported for a lanthanide complex ($\Delta S^{\ddagger} = -30.1 \pm 1$ eu) and for the Zr salicyloxazoline complexes ($\Delta S^{\ddagger} = -13$ to -23 eu). They are, however, rather similar to values reported for a tetravalent U pre-catalyst ($\Delta S^{\ddagger} = -43 \pm 9$ eu) and a (Cp)Zr-bis(oxazolinyl) borate complex ($\Delta S^{\ddagger} = -43 \pm 7$ eu).[5a] The $\Delta H^{\ddagger}$ values obtained in this study were consistent with small changes in bonding at the transition state, while the $\Delta S^{\ddagger}$ values were consistent with a highly ordered transition state.

Interpreting the Experimental and Computational Results

As illustrated in Scheme 8, both monoamido complex **2c** and diamido complex **4a** provide access to the 'catalytically active species' **15**, which seems the best fit to all of the available data. But, the reaction conditions that generate it were very different. Monoamido complex **2c** generates an equivalent of a relatively acidic ammonium salt **B** during the generation of **15**, albeit at a relatively low concentration. This difference in reaction conditions undoubtedly plays a large role in the differences observed in reaction order and KIEs when the reaction is initiated with different pre-catalysts **2c** and **4a**. Such a necessity for two molecules of substrate to form the active catalyst when coupled with a molecule of substrate involved in the inhibition of the catalytically active species (Scheme 6, **20**) gives rise to a net first-order dependence on substrate when monoamido complexes were employed (see above). Alternatively, it may be that the monoamido complexes were not saturating the equilibrium before the turnover limiting step for the monoamido complexes thus generating pseudo-first order kinetics.

In contrast, the diamido complexes were under neutral to mildly basic conditions as 2 equivalents of dimethyl amine are generated in the production of **15**. Since the diamido complexes do not need a second substrate molecule to produce the catalytically active species, one scenario for generating a net zero order in substrate would be – plus one for generating **15** and minus one for inhibition, **20** (see above). An alternative model would be that the diamido precatalysts were evaluated under substrate saturation conditions, which resulted in the zero order dependence. Despite the fact that Me_2NH has a boiling point of 7°C it was clearly observable in the spectra during catalysis (see Fig. S41, Supplementary Material), and, therefore, cannot be assumed to be in the gas phase. Thus it may also be involved in the shuttling of protons between cyclised intermediates **17**, **18**, and **19,** producing a situation that may resemble 'general acid catalysis' regarding the ammonium involved in the protonation when mono-amido pre-catalysts are used.

At catalytic concentrations the amine substrate is roughly 10 to 20 times the concentration of Me_2NH, but for catalysis with diamido complex **4a**, Me_2NH may be expected to be twice the concentration when employing the monoamido complexes. More importantly, ammonium salts are not formed when diamido pre-catalysts are used. In addition, considering the relevant pK_as of Me_2NH (10.73) and, as a surrogate for the substrate, *n*-$BuNH_2$ (10.77), they are of comparable strength although the primary amine is a slightly better base.[12] The acidity of the ammonium salts is most relevant for the monoamido pre-catalyst since it is the ammonium cation that is expected to participate in the protonation steps (**18** → **19**). Whereas, the diamido pre-catalysts do not form the ammonium salts, so it is tempting to invoke the amine pK_as of around the low 40s, until intermediate **18** is given careful consideration. This intermediate also contains a 'tetracoordinated' nitrogen since it is bound to Zr and may be expected to have an enhanced acidity versus the free amine. $Co(en)_3^{3+}$ has a reported acidity of 14.2,[13] which is anticipated to be similar to an amine bound to the Lewis acidic, but neutral, Zr centre. While these pK_a values are based on water measurements, the ammonium values are not expected to differ by more than a few pK_a units in DMSO,[14] but may be 10–13 units higher in acetonitrile.[15] The differences in pK_as is expected to be about the same regardless of the solvent. Yet it is the difference in the transferring agent RNH_3^+, which of necessity undergoes an 'outer sphere' transfer, versus the Zr bound amine (Scheme 8) that likely plays a key role in the difference in reaction order and isotope effect. This difference in proton transfer agents (RNH_3^+ versus RNH_2-Zr) likely gives rise to a significant difference in the symmetry of the proton transfer (RNH_3^+ being much more unsymmetrical) and accounts for the significant difference in the k_H/k_D values.

Summary of Observations

To summarise the key experimental observations that must be accounted for in any mechanism: 1) Hydroamination of primary amine substrates occurred, but secondary amines were not cyclised. 2) Secondary amines were not cyclised even in the presence of a non-cyclisable primary amine thus eliminating the amine-enhanced amido mechanisms. 3) The reaction was first order in monoamido pre-catalyst **2c** and substrate making it second order overall. 4) The reaction was first order in diamido pre-catalyst **4a** and zero-order in substrate making it first order overall. 5) When the amine was deuterated and evaluated for a KIE, complex **2c** was found to have a k_H/k_D of 4.6, and **4a** was found to have a k_H/k_D of 2.4. The difference is attributable to the difference in the acidity and activity of the medium due to the formation of ammonium salts when monoamido complex **2c** was pre-catalyst, since the most acidic species, the ammonium

salt **B** (Scheme 8), will deliver the proton in this case, versus the coordinated amine (**18**, Scheme 6) for the diamido pre-catalyst **4a**. 6) Despite these significant differences the activation parameters, $\Delta H^{\ddagger}$ and $\Delta S^{\ddagger}$, were found to be coincidentally within experimental error of one another. While $\Delta H^{\ddagger}$ was relatively small, 8.7 kcal mol^{-1} for **2c** and 8.3 kcal mol^{-1} for **4a**, which is consistent with small changes in bond enthalpy, the entropy term was large and negative for both, $\Delta S^{\ddagger} = -41$ eu, consistent with a highly ordered transition state. According to the computed free energies of activation as presented in Scheme 6, the turnover limiting step is the protonation of the zircona-azacyclobutane intermediate **18**. This step would be expected to show a primary KIE on the observed order of magnitudes, and is highly ordered incorporating a catalyst and a bicyclic intermediate plus a substrate molecules (coordinated for diamido catalyst **4a** and as the ammonium salt for diiodo catalyst **2c**) to give the large negative $\Delta S^{\ddagger}$ values and small $\Delta H^{\ddagger}$. 7) The coordinately unsaturated catalytically active species **15** is subject to substrate inhibition resulting in a zero order reaction in substrate for pre-catalyst **4a** and first order for pre-catalyst **2c**. 8) A disproportionation of monoamido complexes was considered, but this would make the reaction second order with respect to $[Zr]_0$ (see Supplementary Material), which was not observed. In addition, a disproportionation reaction would make triiodo complex **3c**, which decomposes in the presence of substrate to form imidazolium salt **1c** with observable peaks at 11.55, 9.09, and 8.46 ppm in the ^{1}H NMR spectrum (see above). These peaks are not observed when using complex **2c**. Therefore it was inferred that complex **3c** was not being formed at an observable concentration. Thus the most probable mechanism involves formation of a Zr imido species and an imido-[2 + 2] addition mechanism (Scheme 6) under saturation kinetic conditions in the current study of **4a**.

Conclusions

The possible mechanisms of hydroamination/cyclisation with CCC-NHC Zr complexes have been experimentally and computationally modelled. High temperature ^{1}H NMR data were consistent with decomposition of triiodo complex **3c** into an unidentified Zr species and imidazolium salt **1c**, which accounts for its reported synergistic effect. However, high temperature ^{1}H NMR data were not consistent with the decomposition of complexes **2b** and **4a** into an imidazolium salt when using 1,2-dichlorobenzene as a solvent. Only the [2 + 2] cycloaddition mechanism (Scheme 6) was consistent with the reactivity (no reaction with secondary amino-alkenes even if a primary amino-alkene was present), experimentally observed primary KIE effects, substrate and pre-catalyst orders, and experimentally determined activation parameters.

Experimental

General Procedures

All reactions were performed in an inert atmosphere of N_2 or Ar using a glovebox or standard Schlenk techniques unless otherwise noted. Al_2O_3 (basic, 50–200 μm) was stored in an oven at 150°C before use. Amine substrates were made according to previously reported literature procedures and distilled over CaH_2 before use. ^{1}H and ^{13}C NMR spectra were recorded on 300 or 600 MHz Bruker instruments. CHN combustion analysis was performed by Atlantic Microlabs (Norcross, GA). Chemical shifts (δ) are expressed in ppm and referenced to the residual solvent peak. $Zr(NMe_2)_4$ was freshly sublimed. 1,2-Dichlorobenzene, C_6D_6, and CD_2Cl_2 were dried by passing through a column of activated basic Al_2O_3. Toluene and CH_2Cl_2 were dried using molecular sieves and the SP-1 Solvent System from LC Technology Solutions Inc. 1,3-Bis(imidazol-1′-yl)benzene and 1,3-bis(3′-butylimidazol-1′-yl)benzene diiodide (**1a**) were prepared according to previously reported procedures.[8b,16]

Synthesis and Characterisation

1,3-Bis(3′-hexylimidazol-1′-yl)benzene Diiodide (*1b*)

1,3-Bis(imidazol-1′-yl)benzene (**1**) (3.12 g, 14.7 mmol), 1-iodohexane (45.0 mL, 305 mmol), and CH_3CN (100 mL) were combined in air, degassed, and heated at 120°C for 1 h. The reaction was cooled to room temperature, and concentrated under vacuum yielding a yellow solid. The solid was washed onto a frit with 1 : 1 CH_3CN/Et_2O (50 mL) and washed with additional 1 : 1 CH_3CN/Et_2O (2 × 50 mL). The resulting white solid (7.64 g, 82 %) was dried under vacuum at 110°C overnight. δ_H (DMSO-d_6) 10.01 (s, 2H), 8.45 (s, 2H), 8.38 (s, 1H), 8.15 (s, 2H), 8.05–7.98 (m, 3H), 4.30 (t, 4H, *J* 7.3), 1.93 (m, 4H), 1.315 (m, 12H), 0.87 (t, 6H, *J* 6.6). δ_C (DMSO-d_6) 135.7, 135.6, 131.9, 123.5, 122.6, 121.0, 115.7, 49.6, 30.5, 29.0, 25.1, 21.8, 13.8; HRMS *m/z* 507.1965 $[M - I]^+$, calcd for $C_{24}H_{36}IN_4^+$ 507.1979; 379.2847 $[M - 2I - H]^+$, calcd for $C_{24}H_{35}N_4$ 379.2856.

1,3-Bis(3′-undecyllimidazol-1′-yl)benzene Diiodide (*1c*)

1,3-Bis(imidazol-1′-yl)benzene (**1**) (1.240 g, 5.898 mmol), 1-iodoundecane (5.055 g, 17.91 mmol), and CH_3CN (5 mL) were combined in air, degassed, and heated at 90°C for 5.5 h. During this time, white crystals formed. The reaction was allowed to cool to room temperature. The crystals were collected, washed with acetonitrile (2 × 10 mL) and hexane (5 × 10 mL), and dried under vacuum at 150°C for 24 h (3.429 g, 75 %). δ_H (DMSO-d_6) 10.06 (s, 2H), 8.48 (s, 2H), 8.41 (s, 1H), 8.17 (s, 2H), 8.07–7.95 (m, 3H), 4.31 (t, 4H, *J* 7.1), 1.93 (m, 4H), 1.32–1.23 (m, 34 H), 0.84 (t, 6H, *J* 6.6). δ_C (DMSO-d_6) 135.63, 135.58, 131.9, 123.5, 122.5, 121.0, 115.6, 49.6, 31.2, 29.0, 28.9, 28.7, 28.6, 28.3, 25.5, 22.0, 13.9. HRMS *m/z* 647.3553 $[M - I]^+$, calcd for $C_{34}H_{56}I_4$ 647.3544.

2-(1,3-Bis(3′-hexyl-imidazol-2′-ylidene)phenylene) (dimethylamido)diiodo Zirconium (IV) (*2a*)

$Zr(NMe_2)_4$ (0.248 g, 0.930 mmol), imidazolium salt **1a** (0.559 g, 0.881 mmol), and toluene (25 mL) were heated at 160°C for 4 h. The reaction was allowed to cool to room temperature. A yellow, crystalline solid appeared. The solid was collected, washed with toluene (3 × 5 mL) and Et_2O (5 mL), and dried under vacuum at 100°C overnight (0.368 g, 53 %). δ_H (CH_2Cl_2/C_6D_6) 7.20 (d, 2H, *J* 1.8), 7.06 (t, 1H, *J* 7.8), 6.84 (d, 2H, *J* 7.8), 4.21 (br s, 2H), 4,07 (br s, 2H), 2.76 (br s, 6H), 1.71 (br s, 4H), 1.26–1.12 (m, 12H), 0.73 (t, 6H, *J* 6.7). δ_C (CH_2Cl_2/C_6D_6) 193.6, 164.6, 146.6, 128.9, 121.4, 115.4, 110.3, 52.1, 42.3, 31.77, 31.74, 26.4, 22.8, 14.1. Found: C 40.60, H 5.13, N 8.98. Anal. Calc. for $C_{26}H_{39}I_2N_5Zr$: C 40.73, H 5.13, N 9.14 %.

2-(1,3-Bis(3′-undecyl-imidazol-2′-ylidene)phenylene) (dimethylamido)diiodo Zirconium (IV) (*2b*)

$Zr(NMe_2)_4$ (0.248 g, 0.930 mmol), imidazolium salt **1a** (0.686 g, 0.886 mmol), and toluene (10 mL) were heated at 160°C for 4 h. The reaction was allowed to cool to room temperature. A yellow, crystalline solid appeared. The solid

was collected, washed with toluene (5 mL) and Et_2O (5 mL), and dried under vacuum overnight (0.560 g, 70 %). δ_H (CH_2Cl_2/C_6D_6) 7.23 (d, 2H, *J* 1.8), 7.06 (t, 1H, *J* 7.8), 6.84 (d, 2H, *J* 7.8), 6.82 (d, 2H, *J* 1.8), 4.22 (br s, 2H), 4.07 (br s, 2H), 2.75 (br s, 6H), 1.72 (br s, 4H), 1.19–1.09 (m, 32H), 0.70 (t, 6H, *J* 6.7). δ_C (CH_2Cl_2/C_6D_6) 193.2, 164.2, 146.2, 128.4, 121.0, 114.9, 109.9, 51.7, 41.8, 31.7, 31.4, 29.4, 29.39, 29.33, 29.13, 26.3, 22.5, 13.7. Found: C 47.45, H 6.33, N 7.57. Anal. Calc. for $C_{36}H_{59}I_2N_5Zr$: C 47.68, H 6.56, N 7.72 %.

*2-(1,3-Bis(3′-undecyl-imidazol-2′-ylidene)phenylene) triiodo Zirconium (IV) (**3a**)*

$Zr(NMe_2)_4$ (0.109 g, 0.409 mmol), imidazolium salt **1a** (0.236 g, 0.305 mmol), and toluene (12 mL) were heated at 160°C for 1 h. The reaction was allowed to cool to room temperature and was then stirred under vacuum for 5 min. The flask was refilled with Ar and CH_3I (3.64 g, 25.6 mmol) was added and the mixture was stirred at 90°C for 2 h, after which it was filtered and concentrated to dryness yielding a yellow solid (0.213 g, 71 %). δ_H (C_6D_6) 7.04 (t, 1H, *J* 7.7), 6.56 (d, 2H, *J* 7.8), 6.46 (s, 2H), 5.98 (s, 2H), 4.22 (t, 4H, *J* 7.6), 1.91 (m, 4H), 1.38–1.29 (m, 32 H), 0.90 (t, 6H, *J* 6.9). δ_C (C_6D_6) 196.2, 165.3, 146.6, 129.1, 120.4, 114.8, 110.3, 52.3, 32.4, 31.7, 30.12, 30.07, 30.0, 29.9, 29.7, 26.9, 23.2, 14.4. Found: C 41.20, H 5.26, N 5.63. Anal. Calc. for $C_{34}H_{53}I_3N_4Zr$: C 41.26, H 5.40, N 5.66 %.

*2-(1,3-Bis(3′-butyl-imidazol-2′-ylidene)phenylene) bis(dimethylamido)iodo Zirconium (IV) (**4a**)*

$Zr(NMe_2)_4$ (0.314 g, 1.17 mmol), imidazolium salt **1a** (0.273 g, 0.472 mmol), and THF (3.1 mL) were heated at 120°C for 10 min. The reaction was allowed to cool to room temperature and sit undisturbed overnight. During this time, yellow crystals formed. The mother liquor was decanted. The crystals were washed with hexane (5 × 5 mL) and dried under vacuum (0.191 g, 65 %). δ_H (CH_2Cl_2, 600 MHz) 7.67 (d, 2H, *J* 1.7), 7.42 (t, 1H, *J* 7.8), 7.27 (d, 2H, *J* 1.7), 7.26 (d, 2H, *J* 7.9), 4.01 (t, 4H, *J* 7.4), 3.01 (s, 12 H), 1.78 (m, 4 H), 1.39 (m, 4H), 0.99 (t, 6 H, *J* 7.5). δ_C (CD_2Cl_2, 150 MHz) 189.3, 158.4, 148.8, 132.1, 123.2, 116.7, 111.6, 52.1, 38.5, 34.1, 20.4, 14.1.

*Alternative Synthesis for 2-(1,3-Bis(3′-butyl-imidazol-2′-ylidene)phenylene)bis(dimethyl-amido)iodo Zirconium (IV) (**4a**)*

$Zr(NMe_2)_4$ (0.314 g, 1.17 mmol), imidazolium salt **1a** (0.273 g, 0.472 mmol), and THF (2.5 mL) were heated at 120°C for 10 min. The reaction was allowed to cool to room temperature and sit undisturbed for 13 days. During this time, large yellow crystals formed. The mother liquor was decanted. The crystals were washed with hexane (5 × 5 mL) and dried under vacuum (0.292 g, 92 %). Found: C 45.93, H 5.97, N 13.17. Anal. Calc. for $C_{24}H_{37}IN_6Zr$: C 45.92, H 5.94, N 13.39 %.

Representative Kinetic Run

The temperature inside a preheated ^1H NMR probe was calibrated with an 80 % ethylene glycol/DMSO-d_6 standard and T_1 relaxation values were determined for relevant resonances from the standard (1,3,5-trimethoxybenzene) and substrate **5** via the inverse recovery method. A standard solution of pre-catalyst **2b** (0.0091 M) and 1,3,5-trimethoxybenzene (0.066 M) in 1,2-dichlorobenzene/C_6D_6 (13 : 1) was prepared and its density measured ($d = 1.258$ g mL^{-1}). Substrate **5** (0.0444 g, 0.00604 mmol) and the standard solution (0.835 g) were combined in a screw cap NMR tube. The volume of the total solution was measured and the resulting solution placed in the preheated and calibrated NMR probe. The recycle delay (D1) was set to 5 × the longest T_1 and spectra were collected at regular time intervals after waiting 10 min to allow for temperature equilibration.

Computational Methods

Computational models of the catalyst were created based on the X-ray crystal structure of the CCC-NHC pincer diiodo Zr complex.[17] In some cases, for computational convenience, the *n*-butyl groups were trimmed to methyl groups. The 2,2-dimethylpent-4-en-1-amine substrate was used. Geometries were optimized using the *Gaussian09*[18] implementation of PBEPBE[19] density functional theory.[20] The LANL2DZ basis set and effective core potential (ECP),[21] as modified by Couty and Hall,[22] was utilised for zirconium. The LANL2DZ(d,p) basis set/ECP combinations were used for iodine, bromine, and chlorine.[23] The 6–31G(d') basis sets[24] were utilised for carbon and nitrogen (which have the d polarisation functions taken from the 6–311G(d) basis sets,[25] rather than the default value of 0.8 used in the 6–31G(d) basis sets), and the 6–31G basis set[26] was utilised for hydrogen. Each geometry was optimised in the gas phase and determined to be a minimum energy species or a transition state using an analytical frequency calculation. Standard statistical mechanics relationships for an ideal gas at 1 atm and 298 K were used to determine thermodynamic corrections. For comparison purposes, additional SMD SCRF single-point computations[27] were performed on the optimised geometries using parameters consistent with toluene as the solvent; these results yielded qualitatively similar results to those from the gas phase and are not discussed further. Relative free energy values include a correction to account for the relatively high substrate concentration under experimental conditions. Using the relationship between free energy and the equilibrium constant, $\Delta G = -RT\ln K$, where K was the substrate-to-catalyst ratio of 20, one obtains a concentration correction factor of -1.77 kcal mol^{-1} for 298 K. Reported free energies are gas-phase, concentration corrected values at 298 K.

Supplementary Material

Spectroscopic data (^1H and ^{13}C NMR, and/or exact mass spectra) for the salts, Zr complexes, various experimental and kinetic runs, and plots of kinetic data, and appendices of computational and experimental details are available on the Journal's website.

Acknowledgements

The authors gratefully acknowledge the National Science Foundation (NSF OIA-1539035, NSF EPSCoR EPS-0903787, NSF CHE-0809732, and NSF CHE-0955723), the Department of Education (GAANN-P200A120046), The University of Memphis High Performance Computing Facility, and the Mississippi State University Department of Chemistry and Office of Research and Economic Development for funding. K.N.L. conducted the computational studies, and W.D.C. conducted the experimental studies. The contributions of each coauthor were equally important for publication.

References

[1] (a) D. O'Hagan, *Nat. Prod. Rep.* **2000**, *17*, 435. doi:10.1039/A707613D
(b) T. Robinson, in *The Biochemistry of Alkaloids* (Eds A. Kleinzeller, G. F. Springer, H. G. Wittmann) **1981**, pp. 35–57 (Springer-Verlag: New York, NY).

(c) F. X. Felpin, J. Lebreton, *Eur. J. Org. Chem.* **2003**, 3693. doi:10.1002/EJOC.200300193
[2] T. E. Müller, *Chem. Rev.* **1998**, *98*, 675. doi:10.1021/CR960433D
[3] The value of ~42 kcal mol^{-1} came from calculations completed in this work. See the experimental section and Supplementary Material.
[4] (a) F. Pohlki, S. Doye, *Chem. Soc. Rev.* **2003**, *32*, 104. doi:10.1039/B200386B
(b) D. C. Leitch, R. H. Platel, L. L. Schafer, *J. Am. Chem. Soc.* **2011**, *133*, 15453. doi:10.1021/JA202448B
(c) A. L. Gott, A. J. Clarke, G. J. Clarkson, P. Scott, *Chem. Commun.* **2008**, 1422. doi:10.1039/B718373A
(d) D. C. Leitch, P. R. Payne, C. R. Dunbar, L. L. Schafer, *J. Am. Chem. Soc.* **2009**, *131*, 18246. doi:10.1021/JA906955B
(e) R. K. Thomson, J. A. Bexrud, L. L. Schafer, *Organometallics* **2006**, *25*, 4069. doi:10.1021/OM060545N
(f) L. E. N. Allan, G. J. Clarkson, D. J. Fox, A. L. Gott, P. Scott, *J. Am. Chem. Soc.* **2010**, *132*, 15308. doi:10.1021/JA106588M
(g) V. M. Arredondo, S. Tian, F. E. McDonald, T. J. Marks, *J. Am. Chem. Soc.* **1999**, *121*, 3633. doi:10.1021/JA984305D
(h) M. R. Gagne, T. J. Marks, *J. Am. Chem. Soc.* **1989**, *111*, 4108. doi:10.1021/JA00193A056
(i) D. A. Watson, M. Chiu, R. G. Bergman, *Organometallics* **2006**, *25*, 4731. doi:10.1021/OM0606791
(j) L. Ackermann, R. Bergman, *Org. Lett.* **2002**, *4*, 1475. doi:10.1021/OL0256724
(k) M. R. Douglass, M. Ogasawara, S. Hong, M. V. Metz, T. J. Marks, *Organometallics* **2002**, *21*, 283. doi:10.1021/OM0104013
(l) P. J. Walsh, A. M. Baranger, R. G. Bergman, *J. Am. Chem. Soc.* **1992**, *114*, 1708. doi:10.1021/JA00031A026
(m) L. Ackermann, *Org. Lett.* **2005**, *7*, 439. doi:10.1021/OL047649J
(n) J. Y. Kim, T. Livinghouse, *Org. Lett.* **2005**, *7*, 1737. doi:10.1021/OL050294Z
(o) P. L. McGrane, M. Jensen, T. Livinghouse, *J. Am. Chem. Soc.* **1992**, *114*, 5459. doi:10.1021/JA00039A087
(p) P. L. McGrane, T. Livinghouse, *J. Am. Chem. Soc.* **1993**, *115*, 11485. doi:10.1021/JA00077A053
(q) P. D. Knight, I. Munslow, P. N. O'Shaughnessy, P. Scott, *Chem. Commun.* **2004**, 894. doi:10.1039/B401493F
(r) D. V. Gribkov, K. C. Hultzsch, F. Hampel, *Chem. – Eur. J.* **2003**, *9*, 4796. doi:10.1002/CHEM.200304975
(s) A. L. Reznichenko, T. J. Emge, S. Audörsch, E. G. Klauber, K. C. Hultzsch, B. Schmidt, *Organometallics* **2011**, *30*, 921. doi:10.1021/OM1011006
[5] (a) B. D. Stubbert, T. J. Marks, *J. Am. Chem. Soc.* **2007**, *129*, 6149. doi:10.1021/JA0675898
(b) J. A. Bexrud, J. D. Beard, D. C. Leitch, L. L. Schafer, *Org. Lett.* **2005**, *7*, 1959. doi:10.1021/OL0503992
(c) K. Manna, S. Xu, A. D. Sadow, *Angew. Chem. Int. Ed.* **2011**, *50*, 1865. doi:10.1002/ANIE.201006163
(d) K. Manna, W. C. Everett, G. Schoendorff, A. Ellern, T. L. Windus, A. D. Sadow, *J. Am. Chem. Soc.* **2013**, *135*, 7235. doi:10.1021/JA4000189
(e) A. R. Smith, H. M. Lovick, T. Livinghouse, *Tetrahedron Lett.* **2012**, *53*, 6358. doi:10.1016/J.TETLET.2012.09.019
[6] (a) S. Tobisch, *Dalton Trans.* **2012**, *41*, 9182. doi:10.1039/C2DT30814B
(b) S. Tobisch, *Chem. – Eur. J.* **2012**, *18*, 7248. doi:10.1002/CHEM.201103620
(c) S. Tobisch, *Inorg. Chem.* **2012**, *51*, 3786. doi:10.1021/IC202753M
[7] H. U. Valle, G. Akurathi, J. Cho, W. D. Clark, A. Chakraborty, T. K. Hollis, *Aust. J. Chem.* **2016**, *69*, 565. doi:10.1071/CH15795
[8] (a) W. D. Clark, J. Cho, H. U. Valle, T. K. Hollis, E. J. Valente, *J. Organomet. Chem.* **2014**, *751*, 534. doi:10.1016/J.JORGANCHEM.2013.11.001
(b) J. Cho, T. K. Hollis, E. J. Valente, J. M. Trate, *J. Organomet. Chem.* **2011**, *696*, 373. doi:10.1016/J.JORGANCHEM.2010.10.004
(c) J. Cho, T. K. Hollis, T. R. Helgert, E. J. Valente, *Chem. Commun.* **2008**, 5001. doi:10.1039/B805174G
[9] H. Kitahara, H. Sakurai, *Chem. Lett.* **2010**, *39*, 46. doi:10.1246/CL.2010.46
[10] R. D. Rogers, R. V. Bynum, J. L. Atwood, *J. Am. Chem. Soc.* **1978**, *100*, 5238. doi:10.1021/JA00484A069
[11] (a) I. Prochnow, P. Zark, T. Müller, S. Doye, *Angew. Chem. Int. Ed.* **2011**, *50*, 6401. doi:10.1002/ANIE.201101239
(b) A. L. Reznichenko, F. Hampel, K. C. Hultzsch, *Chem. – Eur. J.* **2009**, *15*, 12819. doi:10.1002/CHEM.200902229
(c) A. Mukherjee, T. K. Sen, P. K. Ghorai, P. P. Samuel, C. Schulzke, S. K. Mandal, *Chem. – Eur. J.* **2012**, *18*, 10530. doi:10.1002/CHEM.201200868
[12] See p. D-159 in: R. C. Weast, *CRC Handbook of Chemistry and Physics* (67th edn) **1986** (CRC Press, Inc.: Boca Raton, FL).
[13] (a) G. Navon, R. Panigel, D. Meyerstein, *Inorg. Chim. Acta* **1972**, *6*, 299. doi:10.1016/S0020-1693(00)91802-4
(b) J. Wilinski, R. J. Kurland, *Inorg. Chem.* **1973**, *12*, 2202. doi:10.1021/IC50127A059
[14] F. G. Bordwell, *Acc. Chem. Res.* **1988**, *21*, 456. doi:10.1021/AR00156A004
[15] R. Schwesinger, H. Schlemper, C. Hasenfratz, J. Willaredt, T. Dambacher, T. Breuer, C. Ottaway, M. Fletschinger, J. Boele, H. Fritz, D. Putzas, H. W. Rotter, F. G. Bordwell, A. V. Satish, G. Z. Ji, E. M. Peters, K. Peters, H. G. Von Schnering, L. Walz, *Liebigs Ann.* **1996**, 1055.
[16] W. D. Clark, G. E. Tyson, T. K. Hollis, H. U. Valle, E. J. Valente, A. G. Oliver, M. P. Dukes, *Dalton Trans.* **2013**, *42*, 7338. doi:10.1039/C3DT32862G
[17] R. J. Rubio, G. T. S. Andavan, E. B. Bauer, T. K. Hollis, J. Cho, F. S. Tham, B. Donnadieu, *J. Organomet. Chem.* **2005**, *690*, 5353. doi:10.1016/J.JORGANCHEM.2005.05.007
[18] M. J. Frisch, G. W. Trucks, H. B. Schlegel, G. E. Scuseria, M. A. Robb, J. R. Cheeseman, G. Scalmani, V. Barone, B. Mennucci, G. A. Petersson, H. Nakatsuji, M. Caricato, X. Li, H. P. Hratchian, A. F. Izmaylov, J. Bloino, G. Zheng, J. L. Sonnenberg, M. Hada, M. Ehara, K. Toyota, R. Fukuda, J. Hasegawa, M. Ishida, T. Nakajima, Y. Honda, O. Kitao, H. Nakai, T. Vreven, J. A. Montgomery, Jr, J. E. Peralta, F. Ogliaro, M. Bearpark, J. J. Heyd, E. Brothers, K. N. Kudin, V. N. Staroverov, R. Kobayashi, J. Normand, K. Raghavachari, A. Rendell, J. C. Burant, S. S. Iyengar, J. Tomasi, M. Cossi, N. Rega, J. M. Millam, M. Klene, J. E. Knox, J. B. Cross, V. Bakken, C. Adamo, J. Jaramillo, R. Gomperts, R. E. Stratmann, O. Yazyev, A. J. Austin, R. Cammi, C. Pomelli, J. W. Ochterski, R. L. Martin, K. Morokuma, V. G. Zakrzewski, G. A. Voth, P. Salvador, J. J. Dannenberg, S. Dapprich, A. D. Daniels, Ö. Farkas, J. B. Foresman, J. V. Ortiz, J. Cioslowski, D. J. Fox, *Gaussian 09 Revision A.02* **2009** (Gaussian, Inc.: Wallingford, CT).
[19] (a) J. P. Perdew, K. Burke, M. Ernzerhof, *Phys. Rev. Lett.* **1996**, *77*, 3865. doi:10.1103/PHYSREVLETT.77.3865
(b) J. P. Perdew, K. Burke, M. Ernzerhof, *Phys. Rev. Lett.* **1997**, *78*, 1396. doi:10.1103/PHYSREVLETT.78.1396
[20] R. G. Parr, W. Yang, *Density-Functional Theory of Atoms and Molecules* **1989** (Oxford University Press: Oxford).
[21] P. J. Hay, W. R. Wadt, *J. Chem. Phys.* **1985**, *82*, 270. doi:10.1063/1.448799
[22] M. Couty, M. B. Hall, *J. Comput. Chem.* **1996**, *17*, 1359. doi:10.1002/(SICI)1096-987X(199608)17:11<1359::AID-JCC9>3.0.CO;2-L
[23] C. E. Check, T. O. Faust, J. M. Bailey, B. J. Wright, T. M. Gilbert, L. S. Sunderlin, *J. Phys. Chem. A* **2001**, *105*, 8111. doi:10.1021/JP011945L
[24] P. C. Hariharan, J. A. Pople, *Theor. Chim. Acta* **1973**, *28*, 213. doi:10.1007/BF00533485
[25] R. Krishnan, J. S. Binkley, R. Seeger, J. A. Pople, *J. Chem. Phys.* **1980**, *72*, 650. doi:10.1063/1.438955
[26] W. J. Hehre, R. Ditchfield, J. A. Pople, *J. Chem. Phys.* **1972**, *56*, 2257. doi:10.1063/1.1677527
[27] A. V. Marenich, C. J. Cramer, D. G. Truhlar, *J. Phys. Chem. B* **2009**, *113*, 6378. doi:10.1021/JP810292N